Guam Comprehensive Flood Study – Part 3

Flood Hazard Study
Nelansa (Manell) River

Merizo Village, Guam

Final Report
31 March 2020

Prepared by:
U.S. Army Corps of Engineers, Honolulu District

Prepared for:
Government of Guam, Bureau of Statistics and Plans

This page is intentionally blank.

Executive Summary

The Guam Comprehensive Flood Study represents a collaborative approach between the US Army Corps of Engineers (USACE) and the Government of Guam to understand flooding hazards across the island. The technical work done by USACE is meant to serve as the planning framework that the Government of Guam will use to work toward reducing flood risk for its communities.

The purpose of the study is to provide the Government of Guam with 1) an update of the regional flood frequency analysis for southern Guam; 2) site-specific hydrologic and hydraulic analysis of two to four flood prone areas within the inventory; and 3) preliminary flood mitigation design concepts for the aforementioned sites. Documentation for the study was divided into four parts:

Part 1 – Flood Frequency Estimates for Streams on Guam

Part 2 – Flood Hazard Study for Umatac River, Guam

Part 3 – Flood Hazard Study for Nelansa (Manell) River, Guam

Part 4 – Flood Hazard Study for Upper Namo River, Guam

This document presents information on Part 3, the objective of which is to 1) provide estimates of the magnitudes of the 50%, 20%, 10%, 4%, 2%, 1%, and 0.2% Annual Exceedance Probability (AEP) peak stream discharges at Nelansa (Manell) River, 2) provide inundation maps representing existing conditions in the floodplain for the 1% and 0.2% AEP flood events, and 3) provide site-specific preliminary flood mitigation design concepts to address flooding caused by Nelansa (Manell) River.

Two different methods were used to estimate the peak flow for the 8 frequency events: 1) rainfall-runoff modeling and 2) regional regression equations as introduced in Part 1 of this study. The peak flow estimates computed by the rainfall-runoff model (Table 4-13) were determined to be the most reliable dataset as it was based on site-specific basin characteristics and calibrated to historical streamflow data from a similar watershed. These flows were used as input for the hydraulic model.

A one-dimensional, steady flow model was created using the Hydrologic Engineering Center's River Analysis System (HEC-RAS) software. Field measurements and observations made during the October 2018 site visit were incorporated into the geometry of the HEC-RAS model. Modeling results indicate floodwaters enter the overbank areas and residential properties as frequently as the 50% AEP (2-yr) event due to the narrow channel, low overbanks, and structural constrictions along the river. The 1% AEP (100-yr) inundation map is presented in Appendix A.

Flood mitigation alternatives specific to this site include: 1) reforestation, 2) restoring the natural flow path, and 3) an upper detention basin. Frequent fires in the watershed have resulted in the native ravine forest being replaced with the more resilient and fire-adapted savannah grass. Savannah grass burns easily, but the roots remain alive and soon after an area burns over it sprouts again. Although the risk of fire and resulting bare soil is higher with savannah grass, its ability to quickly recover limits the time the soil is exposed. Small trees are often killed entirely when burned. In the short term, the savannah grass may be helping to reduce overland flow and sediment runoff by providing immediate cover to otherwise bare soil. However, with each fire, the organic component of the soil is eroded and the ability for any type of vegetation to maintain its existence is lost, resulting in "badland" areas of bare soil. Even the savannah grasses would be unable to grow in these badland areas. Long term effects from burning and the creation of badlands are a real threat in terms of flood risk. The estimated cost of construction to reforest a 1 acre site is approximately $51,400 with a 43% contingency for a total estimated construction contract cost of $73,600.

The intent of the second alternative is to restore the river to a somewhat natural flow path instead of forcing the water to make such a sharp turn in a developed area. While restoring it to its historical path exactly would require extensive work beyond what is necessary to reduce flood risk in the area, constructing a new culvert at the turning point and excavating through the bay front wetland to create a new outflow point would allow flood waters to drain from the area more effectively. Regulatory and permitting actions should be limited as the proposed alternative is the *removal* of fill in the wetland rather than the *placement* of fill. It should be noted that this alternative by itself does not mitigate for the 1% AEP (100-year) peak discharge at this location. It was designed to be cost effective, but by doing so, only mitigates for the 20% AEP (5-year) event. It also assumes that the channel that runs parallel to Route 4 could still be utilized (left in place). The estimated cost of construction to restore the natural flow path of the channel is approximately $387,000 with a 35% contingency for a total estimated construction contract cost of $523,000.

Detention basins can be effective in reducing peak flow by capturing large amounts of water during a storm event and releasing it more gradually. In the Merizo Watershed, there are two possible locations for a detention basin: upstream of Route 4 along the Manell River and between Joutan Lane and J Baza Street. These locations are intended to capture flow from the Manell River and overland runoff from the mountains between the Manell River and Achang Bay, respectively. This would contain nearly the 50% AEP (2 year) flood event and reduce the 10% AEP (10 year) peak flow in half along the Manell River. The estimated cost of construction to retrofit two detention basins is approximately $24,800 with a 43% contingency for a total estimated construction contract cost of $35,500.

TABLE OF CONTENTS

1. INTRODUCTION **3**
1.1 AUTHORITY 3
1.2 PURPOSE AND SCOPE 3
1.3 PARTNER AGENCY 4
1.4 SITE VISIT 4
2. WATERSHED DESCRIPTION **5**
2.1 LOCATION 5
2.2 TOPOGRAPHY 6
2.3 GEOLOGY 6
2.4 SOILS 6
2.5 VEGETATION 6
2.6 CLIMATE 7
2.6.1 El Niño Years 7
3. GEOGRAPHIC INFORMATION SYSTEMS DATA **9**
3.1.1 Datum and Projection 9
3.1.2 Elevation 9
3.1.3 Imagery 10
3.1.4 Digital Atlases of Guam 10
4. HYDROLOGIC ANALYSIS **11**
4.1 RAINFALL-RUNOFF MODELING 11
4.1.1 River Delineation 11
4.1.2 Subbasin Delineation 15
4.1.3 Subbasin Loss Parameterization 16
4.1.4 Subbasin Baseflow 19
4.1.5 Model Calibration 19
4.1.6 Rainfall Frequency Data 21
4.1.7 Hydrologic Model Results 22
4.2 REGIONAL REGRESSION EQUATIONS 22

4.3 REFERENCE FLOWS 23
4.3.1 2007 FIS.. 23
4.4 ADOPTED FLOWS 23
5. DEVELOPMENT OF THE HYDRAULIC MODEL 24
5.1 FLOW DATA 24
5.1.1 Boundary Conditions 24
5.2 GEOMETRY DATA 24
5.2.1 Reach 24
5.2.2 Cross-Sections 25
5.2.3 Bridges 28
5.2.4 Lateral Weirs 29
5.2.5 Manning's n 29
5.2.6 Results 30
6. FLOOD MITIGATION ALTERNATIVES 31
6.1 REFORESTATION 31
6.2 RESTORING THE NATURAL FLOW PATH OF THE CHANNEL 32
6.3 UPPER DETENTION BASIN 35
7. REFERENCES 37

APPENDICES

APPENDIX A – Flood Inundation Maps

LIST OF FIGURES

Figure 2-1: Delineated Subbasins of the Nelansa and Tributary Rivers 5
Figure 4-1: HEC-HMS Basin Model 15
Figure 4-2: Sheet Flow, Shallow Concentrated Flow, and Channel Flow Delineated, Nelansa River, Manell Watershed 17
Figure 5-1: Delineated Rivers in HEC-RAS, Nelansa (Manell) River Basin, Merizo 25
Figure 5-2: HEC-RAS River and Cross-Section Layout 27
Figure 5-3: Inundated Areas in HEC-RAS for the 1% AEP (100-yr) Flood Event 30
Figure 6-1: Historic Path of the Nelansa River 33
Figure 6-2: Current, Proposed, and Historical Path of the Nelansa River 34
Figure 6-3: Potential Sites for a Detention Basin 36

LIST OF TABLES

Table 3-1: Elevation Data Type and Sources 9
Table 4-1: Channel Characteristics 12
Table 4-2: Basin Characteristics 15
Table 4-3: Subbasin Loss Parameters 16
Table 4-4: Sheet Flow Characteristics for each Subbasin 16
Table 4-5: Shallow Concentrated Flow Characteristics for each Subbasin 16
Table 4-6: Channel Flow Characteristics for each Subbasin 18
Table 4-7: Initial Time of Concentration for each Subbasin 18
Table 4-8: Initial Storage Coefficients for each Subbasin 19
Table 4-9: Initial and Calibrated Parameters for the La Sa Fua River Basin 20
Table 4-10: Initial and Calibrated Parameters for the Nelansa River Basin, "Principal_DA" Subbasin 20
Table 4-11: Initial and Calibrated Parameters for the Nelansa River Basin, "Tributary_DA" Subbasin 20
Table 4-12: Point Precipitation Frequency Estimates (in mm) 21
Table 4-13: Calibrated Peak Flow Data from HEC-HMS 22
Table 4-14: Peak Flow Data from Regional Regression Equations 22
Table 4-15: Peak flow data from the 2007 FIS by FEMA 23
Table 5-1: Bridge Data as Measured in the Field 28

LIST OF ACRONYMS & ABBREVIATIONS

- % – percent
- A – area; drainage area
- AEP – annual exceedance probability
- BSP – Bureau of Statistics and Plans
- CN – curve number
- D – depth; bank-full depth
- DEM – digital elevation model
- DPW – Department of Public Works
- FCP – flood control project
- FHWA – Federal Highway Administration
- FPMS – Flood Plain Management Services
- ft - feet
- GCMP – Guam Coastal Management Program
- GIS – geographical information systems
- GUVD04 – Guam Vertical Datum of 2004
- HEC – Hydrologic Engineering Center
- HMS – Hydrologic Modeling Software
- IREI – Island Research & Education Initiative
- JALBTCX – Joint Airborne Lidar Bathymetry Technical Center of Expertise
- km – kilometer
- L – length; length of flow path; length of space between cross sections
- LiDAR – Light Detection and Ranging
- m – meter
- mi – miles
- MHHW – mean higher high water
- MLLW – mean lower low water
- MSL – mean sea level
- *n* – Manning's coefficient
- NAD83 – North American Datum of 1983
- NCDC – National Climatic Data Center
- NOAA – National Oceanic and Atmospheric Administration
- NRCS – National Resources Conservation Service
- NSE – Nash-Sutcliffe model efficiency
- OCD – Office of Civil Defense
- OHS – Office of Homeland Security
- PFDS - Precipitation-Frequency Data Server
- R – storage coefficient
- RAS - River Analysis System
- S_0 = mean channel slope
- SSP – Statistical Software Package
- T_c - time of concentration
- TR-55 - Technical Release 55
- U.S. – United States

- USACE – U.S. Army Corps of Engineers
- USDA – U.S. Department of Agriculture
- USGS – U.S. Geological Survey
- UTM – Universal Transverse Mercator
- WERI – Water and Environmental Research Institute of the Western Pacific
- WGS – World Geodetic System
- W.S. – water surface
- XS - HEC-RAS cross section
- yr - year

1. Introduction

1.1 Authority

This study was completed under the authority of the Flood Plain Management Services (FPMS) Program provided by Section 206 of the 1960 Flood Control Act (Public Law 86-645). As amended, the U.S. Army Corps of Engineers (USACE) is to provide a full range of flood risk information, technical services, and planning guidance in support of active floodplain management.

1.2 Purpose and Scope

The Guam Comprehensive Flood Study represents a collaborative approach between the US Army Corps of Engineers (USACE) and the Government of Guam to understand flooding hazards across the island. The technical work done by USACE is meant to serve as the planning framework that the Government of Guam will use to work toward reducing flood risk for its communities.

The purpose of the study is to provide the Government of Guam with 1) an update of the regional flood frequency analysis for southern Guam; 2) site-specific hydrologic and hydraulic analysis of two to four flood prone areas within the inventory; and 3) preliminary flood mitigation design concepts for the aforementioned sites. Documentation for the study was divided into four parts:

Part 1 – Flood Frequency Estimates for Streams on Guam

Part 2 – Flood Hazard Study for Umatac River

Part 3 – Flood Hazard Study for Nelansa (Manell) River

Part 4 – Flood Hazard Study for Upper Namo River

This document presents information on Part 3, the objective of which is to 1) provide estimates of the magnitudes of the 50%, 20%, 10%, 4%, 2%, 1%, and 0.2% Annual Exceedance Probability (AEP) peak stream discharges for the Nelansa (Manell) River, 2) provide inundation maps representing existing conditions in the floodplain for the 1% and 0.2% AEP flood events, and 3) provide site-specific preliminary flood mitigation design concepts to address flooding caused by Nelansa (Manell) River.

1.3 **Partner Agency**

The Government of Guam, Bureau of Statistics and Plans (BSP), Guam Coastal Management Program (GCMP) is designated as the proponent of the study because of their broad coordination authorities and comprehensive planning mandates. Responsible for land and natural resource planning, GCMP is often involved with issues concerning natural hazards that impact the daily lives of Guam's communities. A common issue faced by Guam residents and Government agencies is flooding. What started out as GCMP's work to provide a basic characterization of flooding problems in the village of Merizo, has now grown to a comprehensive technical assessment of major flood prone areas on the Island because of the partnership and resources provided by USACE Honolulu District.

1.4 **Site Visit**

In October 2018, USACE personnel conducted a site visit to measure bridge crossings, take photographs of the channel, and investigate the three priority sites included in the Guam Comprehensive Flood Study. They also met with BSP representatives to understand the unique challenges at each priority site and overall flood history. Several photos included in this report are from that site visit. Bridge and channel measurements were incorporated into the hydraulic model. Site-specific information provided by BSP added value to the development of alternatives for flood mitigation.

2. Watershed Description

2.1 Location

Flooding caused by the Nelansa River, also known as the Manell River, is the focus of this report. The Nelansa River is located in the Manell Watershed and southernmost village of Merizo (Figure 2-1) (Merizo, Guam, 2019).

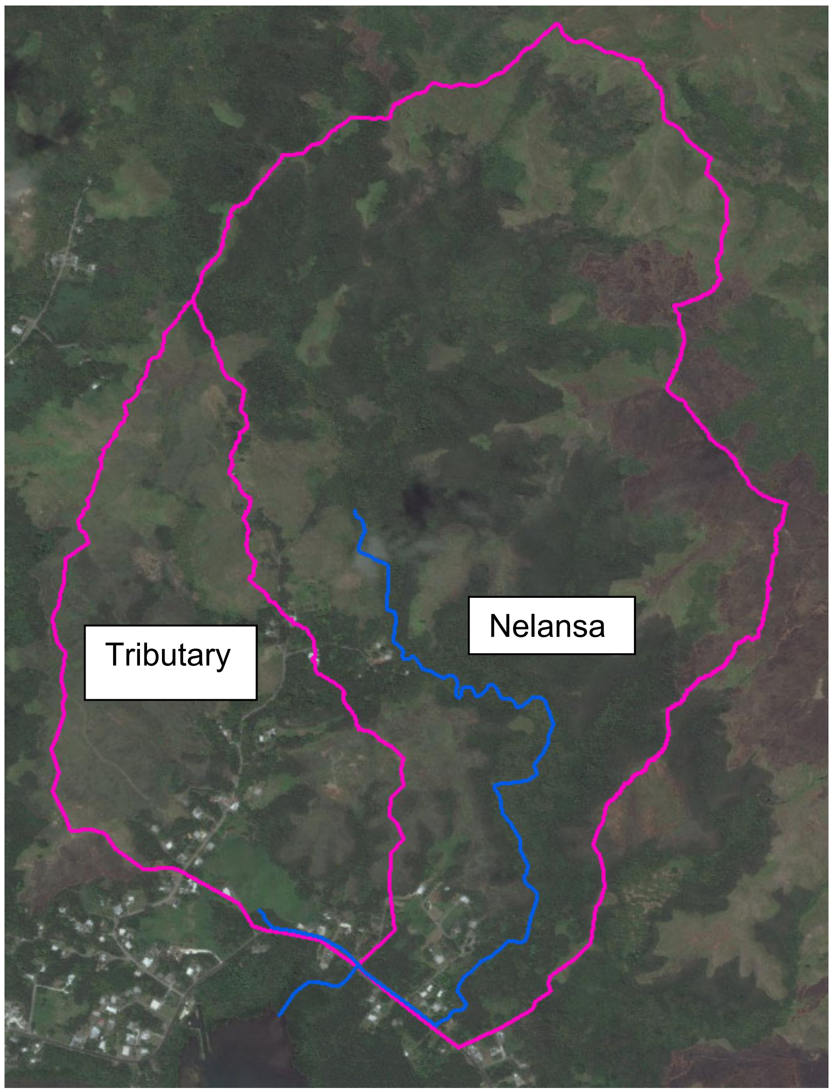

Figure 2-1: Delineated Subbasins of the Nelansa and Tributary Rivers

2.2 **Topography**

The drainage basin for the Nelansa River has an area of about 2.91 square (sq) kilometers (km) [1.13 sq miles (mi)], is approximately 1.7 km (1.0 mi) wide, and 2.6 km (1.6 mi) long, extending from Mount Sasalaguan to Achang Bay. With Mount Sasalaguan approximately 337 meters (m) [1,106 feet (ft)] above sea level, the basin slope is a moderately-steep 13 percent (%). Steep land slopes and soils with a low permeability are often associated with greater stream incision. The longest watercourse in the basin is approximately 3.7 km (2.3 mi) with an approximate channel slope of 1.1%.

2.3 **Geology**

The basin of the Nelansa River (study area) is characterized by rolling to mountains land that is underlain by breccia, conglomerate, sandstone, and shale derived from volcanic rock. These rocks and the alluvial deposits in the stream valley have a low permeability (WERI and IREI, n.d.).

2.4 **Soils**

The soils within the study area primarily belongs to the Akina and Agfayan series, especially in the volcanic uplands (Soil Conservation Service, 1985). These soils are classified as silty clay, volcanic in origin. The soils have moderately slow permeability, resulting in rapid runoff. Erosion is a serious concern for Akina soils, which are characteristically dark reddish brown to dark red in color compared to the Agfayan soils which are black, yellow, or brown (University of Guam, 2016).

Near the coast and lower elevations, the soil primarily belongs to the Inarajan series, which is also a silty clay of volcanic origins. It has a slow permeability rate, seasonal high water table, and is typically a dark gray color. Erosion is not a problem for this soil type (University of Guam, 2016).

2.5 **Vegetation**

In the southern section of Guam, a heavy growth of tropical vegetation borders the inland areas of rivers and represents a plant community known as the ravine forest. Sharp divisions between the non-native savannah grasslands and ravine forest provide particularly aesthetic contrasts in the study area. Fires occur frequently and are often intentionally set by people to draw deer and pigs out when hunting, to clear fields for farming, or as wildfire arson. The spatial extent of the savannah grasslands has increased in size as the fire-adapted grasslands quickly replace the burned forest edge. The southern uplands are some of the island’s only expanses of unspoiled terrain.

2.6 **Climate**

Guam’s climate is tropical marine, reflecting the nearness of the equator and the influence of warm surrounding waters. Wind and rainfall are the most variable elements; humidity, temperature and pressure remain fairly constant. The year is divided into a wet (July through December) and a dry (January through June) season with pronounced differences in rainfall.

Two principal kinds of storms contribute to the climatic character of Guam: small-scale storms, consisting of thunderstorms and squalls, and large systems of tropical storms and typhoons. The small-scale disturbances may dominate an area of only a few square miles. Larger cyclonic storm systems may dominate an area as large as 300,000 square miles and can persist for a week or more.

Major tropical cyclonic disturbances of these kinds occur in all months, but they are prevalent during the rainy season with the greatest probability in the months of October and November. These typhoons are actually tropical storms accompanied by winds of 65 knots (120 kilometers per hour) or greater. Based on the information provided by the Digital Atlas of Southern Guam website, “an average of three tropical storms and one typhoon pass within 180 nautical miles (330 km) of Guam each year” with the most intense typhoon to pass over Guam recently being Super Typhoon Pongsona on December 8, 2002 (WERI and IREI, n.d.).

2.6.1 **El Niño Years**

The term *El Niño* refers to a periodic warming (every two to seven years) of the Pacific Ocean surface waters. These conditions often result in tropical rains shifting eastward across the Pacific and an increased risk of typhoons from March through July and October through December. Rainfall is characteristically greater at the start of El Niño conditions (beginning in May or June), near normal by December, and well below average by the following February. (NOAA Pacific RISA 2015). The duration, strength, and impacts of El Niño events vary, but three periods are universally accepted as having produced very strong conditions: 1982-83, 1997-98, and 2015-16 (NOAA Climate Prediction Center 2018).

3. Geographic Information Systems Data

Several terrain models and data layers were used to perform the hydrologic and hydraulic analysis of the study area. The Geographical Information Systems (GIS) data, sources, and description are summarized in the following sections.

3.1.1 **Datum and Projection**

The datum and projection for this study is as follows:

Horizontal projection: Universal Transverse Mercator (UTM) Zone 55 North (N), meters

Horizontal datum: World Geodetic System 1984 (WGS84)

Vertical Datum: Guam Vertical Datum of 2004 (GUVD04)

Tidal Epoch: 1983 – 2001

3.1.2 **Elevation**

The following sources of elevation data were used in this study:

Table 3-1: Elevation Data Type and Sources

Survey year	Agency	Data type	Location
2012 – 2013	USGS	LiDAR	Island of Guam
2007	JALBTCX	LiDAR	Island of Guam

Light Detection and Ranging (LiDAR) data were collected across the island of Guam by NOAA Office for Coastal Management (OCM) in 2012 and 2013 for the U.S. Geological Survey (USGS). The data is in North Atlantic Datum 1983 (NAD83) MA11, vertically referenced to GUVD04, has a vertical accuracy of +/- 8 centimeters (cm), and horizontal accuracy of +/- 0.11 m. This data was given first priority in creating the merged digital elevation model (DEM) for use in this study.

LiDAR data were also collected by USACE and the Joint Airborne LiDAR Bathymetry Technical Center of Expertise (JALBTCX) in 2007 for the Government of Guam. This data includes hydrographic and topographic data depicting the elevations above and below the immediate coastal water. The topographic lidar data are vertically referenced to Mean Sea Level (MSL) and the bathymetric lidar data are referenced to Mean Lower Low Water (MLLW). The data set has a horizontal accuracy of +/- 0.75 m and a vertical accuracy of

+/- 20 cm. The data was collected so that the horizontal and vertical datum could be specified by the user. For this project, the selected projection was the Universal Transverse Mercator (UTM) coordinate system, zone 55N. Horizontal coordinates reference the NAD83 in meters. The vertical control datum is the Guam Vertical Datum of 2004 (GUVD04), in meters.

3.1.3 **Imagery**

High resolution imagery used for background mapping of the study area is from the National Geospatial-Intelligence Agency and the USGS. World Imagery, provided by Esri, was used for larger scale background mapping, such as when it was necessary to show the entire island of Guam.

3.1.4 **Digital Atlases of Guam**

The Digital Atlas of Southern Guam and the Digital Atlas of Northern Guam, by WERI and IREI, provide public access to geospatial data that covers the entire island of Guam. The website address is: http://south.hydroguam.net/ and http://north.hydroguam.net/. Several files were downloaded and used as a resource for this study, including files on geology, climate, soil, surface water, land cover, and infrastructure.

4. Hydrologic Analysis

Methods for estimating the peak flow for the 50%, 20%, 10%, 4%, 2%, 1%, 0.4%, and 0.2% AEP (2-, 5-, 10-, 25-, 50-, 100-, 250-, and 500-year) flood events (8 profiles) include the following:

1. Rainfall-Runoff Modeling
2. Regional Regression Equations

Other peak flow estimates previously published (for reference):

1. 2007 FEMA FIS

A stream-gage analysis was not performed for this watershed as there are no streamflow gaging stations within the Nelansa (Manell) watershed.

4.1 Rainfall-Runoff Modeling

The hydrologic model was created using the Hydrologic Engineering Center's Hydrologic Modeling System (HEC-HMS) software. This section describes rainfall, riverine, and basin characteristics that were used to create the model, as well as the resulting flow estimates for different probability events.

4.1.1 River Delineation

The principal river (the Nelansa River) was delineated in GIS, extending from the upper watershed to the ocean outlet. This river is primarily a natural and unlined river until it transitions into a concrete-lined drainage ditch that runs parallel to and under Route 4. A tributary from the west was also identified that joins the principal river just above Route 4. Typical channel characteristics are provided in Table 4-1. Photographs showing typical conditions as observed during the October 2018 site visit are presented in Photo 4-1 through Photo 4-4.

Table 4-1: Channel Characteristics

River	Reach	Length (m) [1]	Slope (m/m) [1]	Manning's *n*[1,2]	Bottom Width (m) [2]	Side Slopes (xH:1V) [2]
Nelansa	Natural Channel	2,110	0.012	0.04	6.25	0.5
Nelansa	Concrete Channel	303	0.0085	0.02	3.66	0
Tributary	Natural Swale / Concrete Ditch	186	0.0027	0.02	0.914	0
Nelansa	Natural Channel to Outlet	242	0.00056	0.04	6.25	0.5

[1]: as determined using GIS
[2]: as determined using data collected during the October 2018 site visit

Only the first two reaches of the principal river were determined to be significant enough to include in the hydrologic model (the peak flow is likely to change as water moves down the reach). "Reach-1" in the HEC-HMS model represents the 2,110 m long natural channel of the Nelansa River. "Reach-2" represents the 303 m concrete channel, downstream of "Reach-1."

Photo 4-1: Nelansa (Manell) River, Natural Channel Reach Upstream of Route 4

Photo 4-2: Nelansa (Manell) River, Concrete Channel Reach along Route 4

Photo 4-3: Tributary River, Natural Swale along Route 4

Photo 4-4: Tributary River, Concrete Ditch along Route 4

4.1.2 **Subbasin Delineation**

The corresponding drainage areas that contribute flow to the principal river and tributary were also delineated in GIS. These are referred to as "Principal_DA" and "Tributary_DA" in the HEC-HMS model and this chapter, respectively. The HEC-HMS basin model is provided as Figure 4-1. Table 4-2 identifies the total drainage area and centroid coordinates for each subbasin.

Table 4-2: Basin Characteristics

HEC-HMS Subbasin Name	Area (km^2)	Centroid	
		Latitude	Longitude
Principal_DA	2.31	13.268	144.691
Tributary_DA	0.819	13.264	144.685

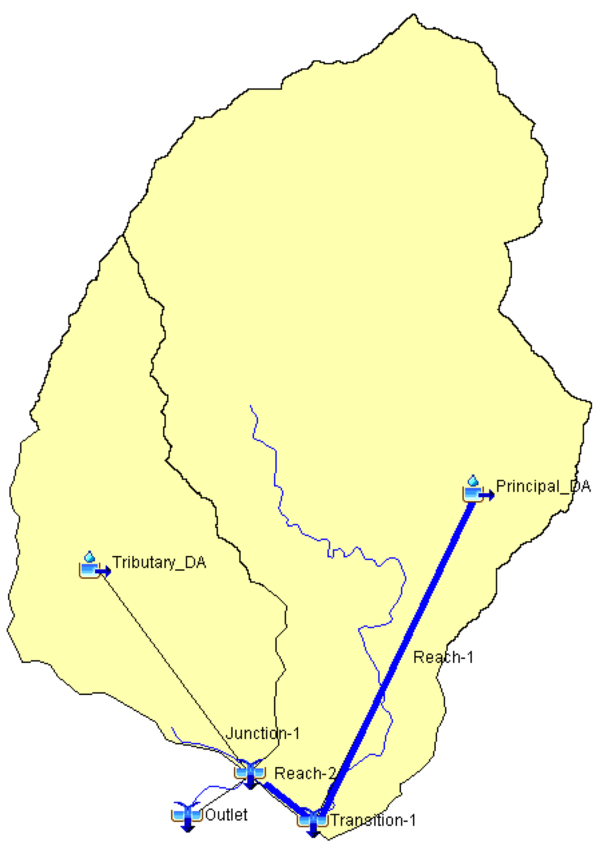

Figure 4-1: HEC-HMS Basin Model

4.1.3 **Subbasin Loss Parameterization**

As described in Section 2.3, Geology, the low-permeability volcanic rocks and alluvial deposits along the streambed slow the infiltration of rainwater. Initial loss was set to 0.1 millimeters (mm), the lowest value accepted by the HEC-HMS program. Constant loss was estimated to be 0.15 mm per hour (hr). The percent impervious was approximated in GIS to be 1% and 3% for the principal and tributary subbasins, respectively.

Table 4-3: Subbasin Loss Parameters

HEC-HMS Subbasin Name	Initial Loss (mm)	Constant Rate (mm/hr)	Impervious (%)
Principal_DA	0.1	0.15	1
Tributary_DA	0.1	0.15	3

Table 4-4: Sheet Flow Characteristics for each Subbasin

HEC-HMS Subbasin Name	Manning's *n*	Sheet Flow Length (m)	Land Slope (m/m)	2-yr, 24-hr Rainfall (mm)	Tc, sheet (hrs)
Principal_DA	0.4	91.4	1.23	150	0.051
Tributary_DA	0.4	48.3	0.379	150	0.030

Table 4-5: Shallow Concentrated Flow Characteristics for each Subbasin

HEC-HMS Subbasin Name	Surface Description	Shallow Flow Length (m)	Watercourse Slope (m/m)	Average Velocity (m/s)	Tc, shallow (hrs)
Principal_DA	Unpaved	269	0.424	3.20	0.023
Tributary_DA	Unpaved	970	0.085	1.46	0.316

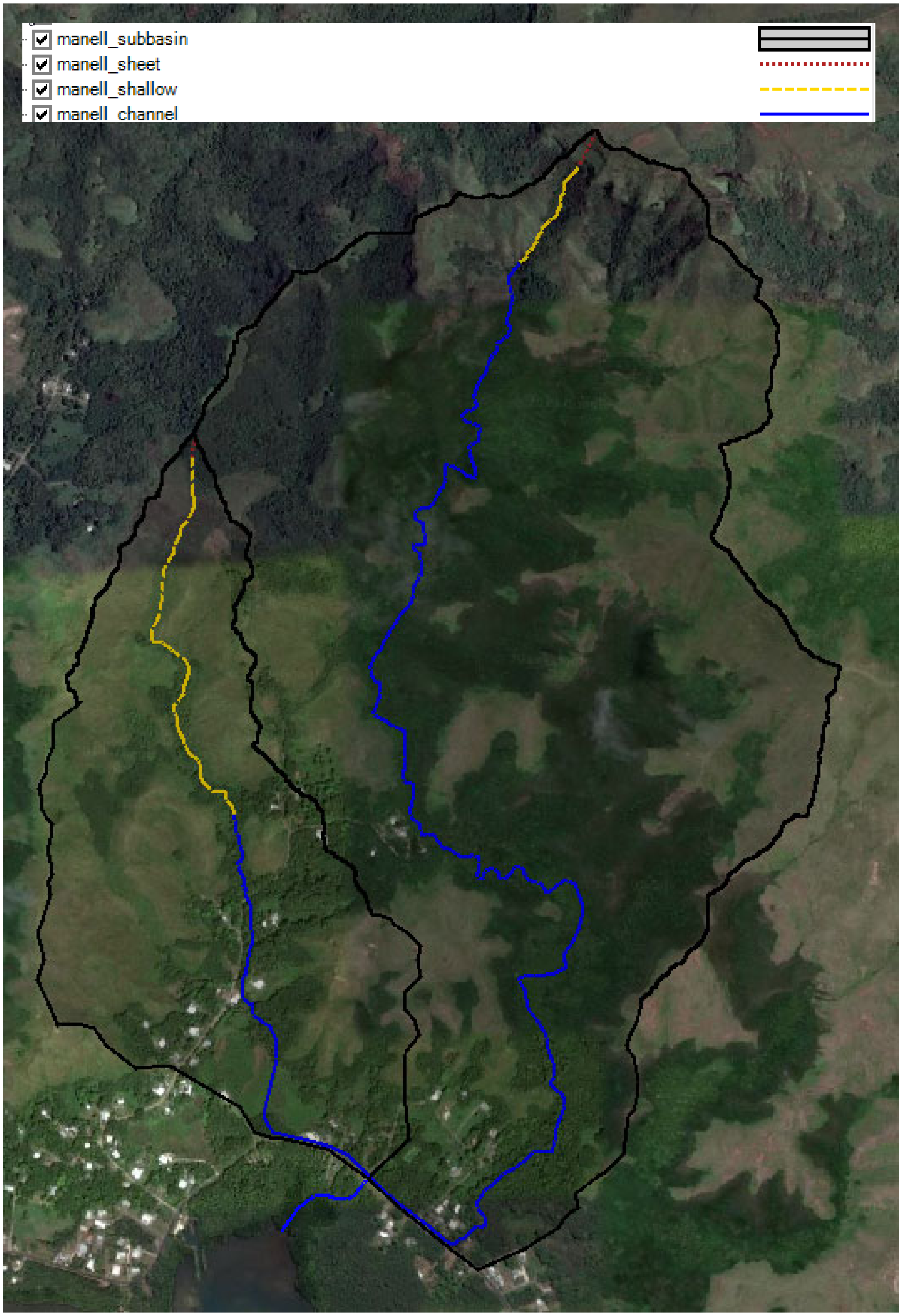

Figure 4-2: Sheet Flow, Shallow Concentrated Flow, and Channel Flow Delineated, Nelansa River, Manell Watershed

Table 4-6: Channel Flow Characteristics for each Subbasin

HEC-HMS Subbasin Name	Hydraulic Radius (m)	Channel Slope (m/m)	Manning's *n* Channel	Velocity (m/s)	Flow Length (m)	Tc, channel (hrs)
Principal_DA[1]	1.49	0.051	0.04	7.38	2,100	0.079
Principal_DA[2]	0.984	0.009	0.02	1.04	249	0.067
Tributary_DA	1.49	0.018	0.04	4.97	1,050	0.059
[1]: Reach-1: Natural Channel [2]: Reach-2: Concrete-Lined Channel						

Table 4-7: Initial Time of Concentration for each Subbasin

HEC-HMS Subbasin Name	Time of Concentration, Tc (hrs)
Principal_DA	0.220
Tributary_DA	0.405

The Clark Unit Hydrograph storage coefficient, R, accounts for storage in the watershed. This parameter was determined using a mathematical relationship between the longest flow path, drainage area, and time of concentration. An equation was adopted from the "Drainage Design Manual for Maricopa County" (Flood Control District of Maricopa County, 2013) for use in this study. This relationship was used to make an initial estimate of the storage coefficient of each sub-basin. These estimates were adjusted during the hydrologic model calibration. The equation used is as follows:

$$R = 0.37{T_c}^{1.11}A^{-0.57}L^{0.80}$$

R: Storage Coefficient

Tc: Time of Concentration (hrs)

A: Drainage Area (square miles)

L: Length of flow path (miles)

The initial values for the storage coefficient parameter are summarized in Table 4-8.

Table 4-8: Initial Storage Coefficients for each Subbasin

HEC-HMS Subbasin Name	Time of Concentration (hrs)	Area (mi^2)	Length of Flow (mi)	Storage Coefficient, R
Principal_DA	0.220	0.891	1.68	0.111
Tributary_DA	0.405	0.316	1.29	0.321

4.1.4 **Subbasin Baseflow**

Neither the principal nor tributary river was observed having flow during the October 2018 site visit. Therefore, baseflow was not included in the hydrologic model.

4.1.5 **Model Calibration**

Although there is no historical stream flow data within the study area, gaged data from a nearby watershed with similar characteristics was used for calibration purposes. Rainfall and stream flow data from the La Sa Fua River, located northwest of the study area, was used to calibrate the sub-basin parameters within the basin of the Nelansa River. As presented in Part 2 – Flood Hazard Study for the Umatac River, the La Sa Fua River Basin was calibrated to 8 different events, ranging from Typhoon Chata’an in July 2002 to Typhoon Mangkhut in September 2018.

The initial parameters for the La Sa Fua River Basin were computed using the same loss and transform methods used for the Nelalnsa River Basin. The initial and final parameters for the La Sa Fua River Basin are presented in Table 4-9:

Table 4-9: Initial and Calibrated Parameters for the La Sa Fua River Basin

Calibration Status	Drainage Area (km)	Initial Loss (mm)	Constant Loss Rate (mm/hr)	Time of Concentration (hr)	Storage Coefficient (hr)
Initial	2.73	0.1	0.15	0.673	0.545
Calibrated	2.73	26	5.81	0.419	0.508
% Change	**0**	**259**	**37.7**	**-0.377**	**-0.069**

Based on the resulting increase in loss parameters and decrease in transform parameters, the initial parameters computed for the Nelansa River Basin were similarly adjusted. The final calibrated parameters for the Nelansa River Basin are shown in Table 4-10 and Table 4-11.

.

Table 4-10: Initial and Calibrated Parameters for the Nelansa River Basin, "Principal_DA" Subbasin

Calibration Status	Drainage Area (km)	Initial Loss (mm)	Constant Loss Rate (mm/hr)	Time of Concentration (hr)	Storage Coefficient (hr)
Initial	2.31	0.1	0.15	0.220	0.111
Calibrated	2.31	26	5.81	0.137	0.103
% Change	**0**	**259**	**37.7**	**-0.377**	**-0.069**

Table 4-11: Initial and Calibrated Parameters for the Nelansa River Basin, "Tributary_DA" Subbasin

Calibration Status	Drainage Area (km)	Initial Loss (mm)	Constant Loss Rate (mm/hr)	Time of Concentration (hr)	Storage Coefficient (hr)
Initial	0.819	0.1	0.15	0.405	0.321
Calibrated	0.819	26	5.81	0.252	0.299
% Change	**0**	**259**	**37.7**	**-0.377**	**-0.069**

4.1.6 **Rainfall Frequency Data**

Point precipitation frequency data were taken from the NOAA's Atlas 14 Precipitation-Frequency Data Server (PFDS) (NOAA, NOAA Atlas 14 Point Precipitation Frequency Estimates, 2017). This source presents rainfall frequencies from recurrence intervals of 1 to 500 years (100% to 0.2% chance exceedance) for sites in Guam. The location points used to extract PFDS data were the approximate centroid locations for each subbasin. The latitude and longitude for these centroids are included in Table 4-2. As the two partial-duration depth curves are nearly identical (an occasional difference of 0.25 mm), one curve will be used to represent both subbasins in the HEC-HMS model (Table 4-12).

Table 4-12: Point Precipitation Frequency Estimates (in mm)

Duration	Average recurrence interval (years)							
	2	5	10	25	50	100	200	500
5 Minutes	14.0	17.2	19.8	23.2	25.9	28.7	31.8	35.6
15 Minutes	27.9	34.5	39.6	46.5	51.8	57.4	63.2	71.4
1 Hour	56.1	69.0	79.0	93.0	104	115	127	142
2 Hours	71.6	88.1	101	119	133	148	163	183
3 Hours	83.6	104	120	141	158	176	194	219
6 Hours	103	133	156	188	213	238	264	302
12 Hours	121	164	198	244	279	318	356	409
1 Day	150	204	247	305	351	399	399	513

4.1.7 **Hydrologic Model Results**

The HEC-HMS model was used to simulate the 50-, 20-, 10-, 4-, 2-, 1-, and 0.2% AEP flood frequency events. The resulting peak discharges for the two subbasins are presented in Table 4-13.

Table 4-13: Calibrated Peak Flow Data from HEC-HMS

HEC-HMS Element Name	Drainage Area (km^2)	Peak Flow (m^3/s)[1]						
		2-yr (50%)	5-yr (20%)	10-yr (10%)	25-yr (4%)	50-yr (2%)	100-yr (1%)	500-yr (0.2%)
Principal_DA	2.31	43.1	59.3	70.7	84.6	94.9	105.5	132
Transition-1	2.31	39.9	54.7	65.0	77.7	87.0	96.6	120
Tributary_DA	0.819	12.3	17.0	20.3	24.3	27.3	30.4	38.0
Junction-1	3.13	51.5	70.9	84.4	101	113	126	157
Outlet	3.13	51.5	70.9	84.4	101	113	126	157
[1]: rounded to three significant figures								

4.2 **Regional Regression Equations**

In Part 1 of this study, regional regression equations were developed for estimating various peak flow magnitudes at ungaged, unregulated sites in southern Guam. These equations were used to estimate peak flow for the principal and tributary drainage basins that contribute flow into the Nelansa (Manell) watershed. The results are presented in Table 4-14.

Table 4-14: Peak Flow Data from Regional Regression Equations

Location		Peak Flow (m^3/s)[1]						
	2-yr (50%)	5-yr (20%)	10-yr (10%)	25-yr (4%)	50-yr (2%)	100-yr (1%)	250-yr (0.4%)	500-yr (0.2%)
Principal_DA Outlet	11.7	12.1	24.4	30.2	39.7	45.7	51.4	61.0
Tributary_DA Outlet	6.53	6.66	13.1	16.1	20.7	23.6	26.2	30.6
[1]: rounded to three significant figures								

4.3 **Reference Flows**

4.3.1 **2007 FIS**

In September 2007, the Federal Emergency Management Agency (FEMA) published Flood Insurance Study (FIS) 660001CV000A for the Territory of Guam (FEMA, 2007). This study includes peak flow estimates for the Nelansa (Manell) River at the mouth and 610 m (2,000 ft) above the mouth (Table 4-15).

Table 4-15: Peak flow data from the 2007 FIS by FEMA

Location	Drainage area (km^2)	Peak flow (m^3/s)[1]			
		1/10	1/50	1/100	1/500
Mouth	0.93	40.8	59.5	68.0	88.6
610 m above mouth	0.8	36.0	52.4	60.0	78.2
[1]: rounded to three significant figures					

4.4 **Adopted Flows**

As the HMS model used site-specific information and was calibrated to historical data from a nearby basin, these peak flows (Table 4-13) are more reliable and should be used as the flow input for the hydraulic model.

5. Development of the Hydraulic Model

The hydraulic model was created using the Hydrologic Engineering Center's River Analysis System (HEC-RAS) software (version 5.0.5, HEC, 2018). The peak flow values determined in Section 4, Hydrologic Analysis were used to represent the amount of water entering the system. Field measurements and observations made during the October 2018 site visit were incorporated into the geometry of the HEC-RAS model. As a result of these efforts, a summary of flood impacts to the site are provided at the end of this section.

5.1 Flow Data

As the Nelansa (Manell) HMS model used site-specific information and was calibrated to historical data, the peak flows computed by the model (Table 4-13) are the most reliable and were used as the flow input for the HEC-RAS model.

5.1.1 Boundary Conditions

"Normal Depth" was the selected upstream boundary condition as flow was considered to be uniform (the slope is not very steep at the upstream boundary). The upstream slope used for normal depth computation was 0.012 for the principal river and 0.015 for the tributary.

"Known W.S" was the selected downstream boundary condition. The mean higher high water (MHHW) from NOAA tidal stations 1630000 Apra Harbor, Guam was used as the known water surface (Known W.S) representing the downstream boundary condition. The MHHW above MSL (as the terrain data is in m above MSL) at this station is 0.26 m above MSL (or 0.85 ft MSL) (NOAA, Datums for 1630000, Apra Harbor, Guam , 2018).

5.2 Geometry Data

5.2.1 Reach

The extent of the Nelansa (Manell) River included in the HEC-RAS model is from the ocean outlet to 1,400 m upstream. The extent of the Tributary River is from the junction with the Nelansa (Manell) River to 230 m upstream. The delineated river is shown in Figure 5-1.

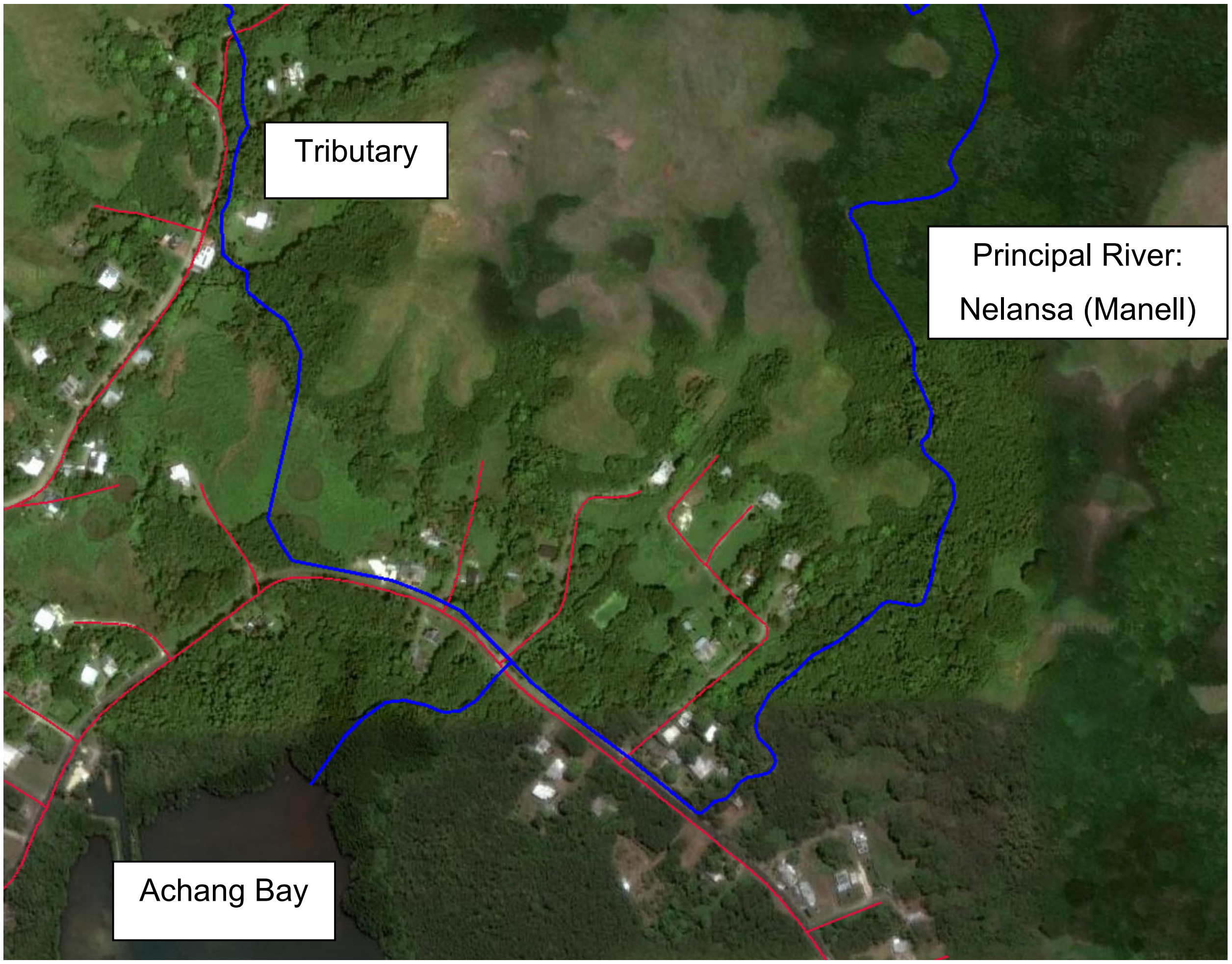

Figure 5-1: Delineated Rivers in HEC-RAS, Nelansa (Manell) River Basin, Merizo

5.2.2 **Cross-Sections**

Cross-sections were drawn at varying intervals along the river to characterize the flow carrying capability of the river and its adjacent floodplain (see Figure 5-2). A terrain was created in HEC-RAS based on the Light Detection and Ranging (LiDAR) data collected in 2007. Initial elevations for each cross-section were extracted from this terrain and then adjusted, as needed, to reflect measurements taken in the field during the October 2018 site visit. Such measurements include typical channel dimensions as previously presented in

Table 4-1, as well as bridge and culvert dimensions, presented in Section 5.2.3.

An average cross-section spacing of 25 meters was used, which is appropriate for the Nelansa (Manell) River. This was determined using Samuel's equation:

$$L = \frac{0.15D}{S_o}$$

where,

L: Spacing of cross sections (m)

D: Bank fill depth (m)

S_o: Mean Channel Slope (m/m)

The Nelansa (Manell) River has a typical bank fill depth of 2 meters and mean channel slope of 0.012.

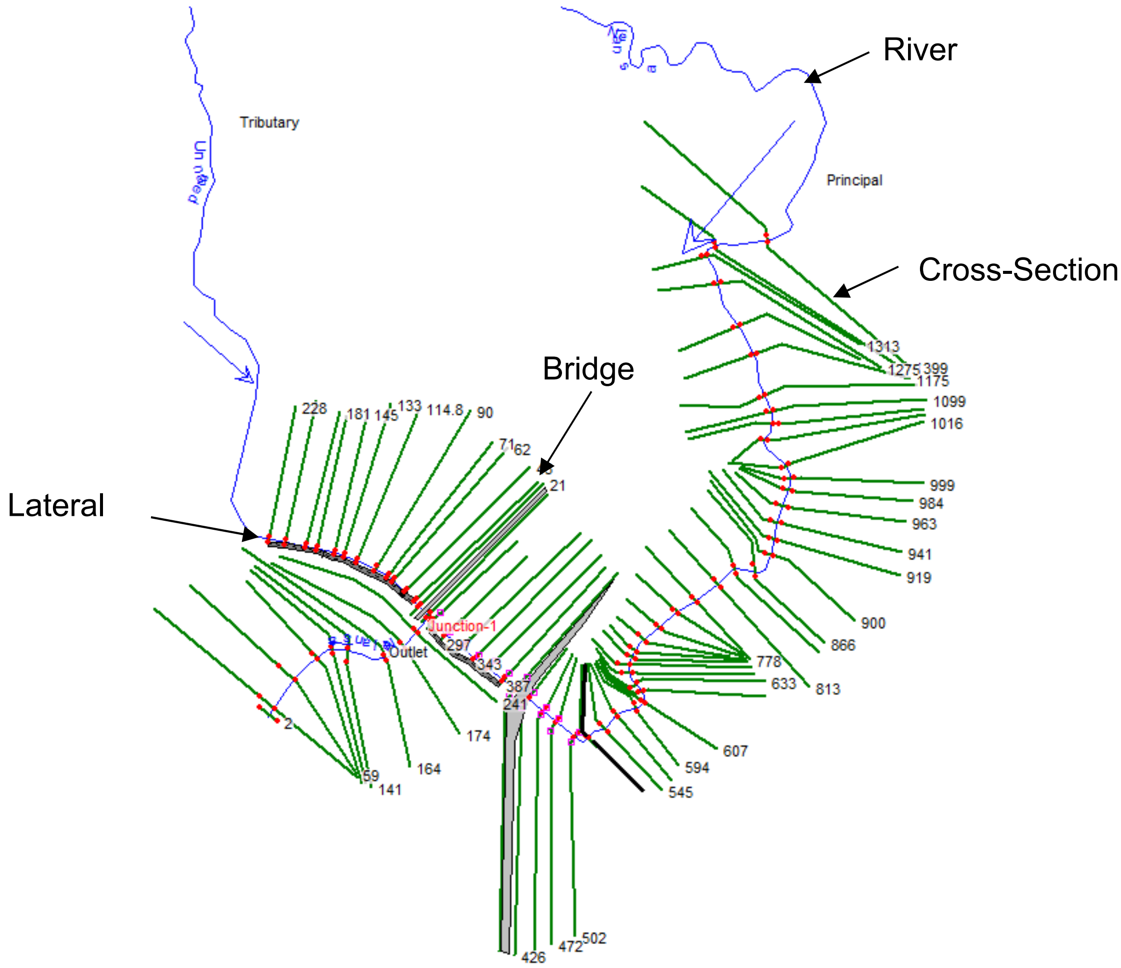

Figure 5-2: HEC-RAS River and Cross-Section Layout

5.2.3 **Bridges**

Two bridges were included in the model, one crossing the principal river at HEC-RAS cross-section (XS) 415 (Photo 5-1), and one crossing the unnamed tributary at XS 15 (Photo 5-2). Bridge data, as measured in the field during the October 2018 site visit, is presented in Table 5-1.

Table 5-1: Bridge Data as Measured in the Field

River	XS	Culvert Data			Pier Width (m)	Headwall Height (m)	Deck Width (m)
		#	Span (m)	Rise (m)			
Principal	415	3	1.83	1.34	0.152	1.19	11.3
Tributary	15	3	1.83	0.762	0.152	1.19	7.2

Photo 5-1: Bridge over Nelansa (Manell) River at XS 415

Photo 5-2: Bridge over Unnamed (Tributary) River at XS 15

5.2.4 **Lateral Weirs**

Route 4 was represented in the HEC-RAS model as two lateral weirs, one for the principal river and one for the tributary river. The culverts that pass underneath Route 4 were also represented by the weir. A weir coefficient of 0.55 was used to represent flow over a roadway (Goodell, Lateral Structure Coefficients, 2013).

5.2.5 **Manning's n**

In the HEC-RAS model, a Manning's roughness coefficient, *n*, is required for the main channel, left overbank, and right overbank areas. As presented in Section 4.1.1, the Manning's *n* for the concrete-lined channel and natural channel were 0.02 and 0.04, respectively. Overbank areas were represented by four types of land cover: evergreen forest (0.16), forested wetland (0.12), grassland (0.035), and developed open spaces (0.04).

5.2.6 **Results**

The narrow channel, short overbanks, and structural constrictions along both the principal and tributary rivers result in floodwaters entering the overbank areas and residential properties as frequently as the 50% AEP (2-yr) event. The inundation map generated by the HEC-RAS model for the 1% AEP (100-yr) event is presented as Figure 5-3.

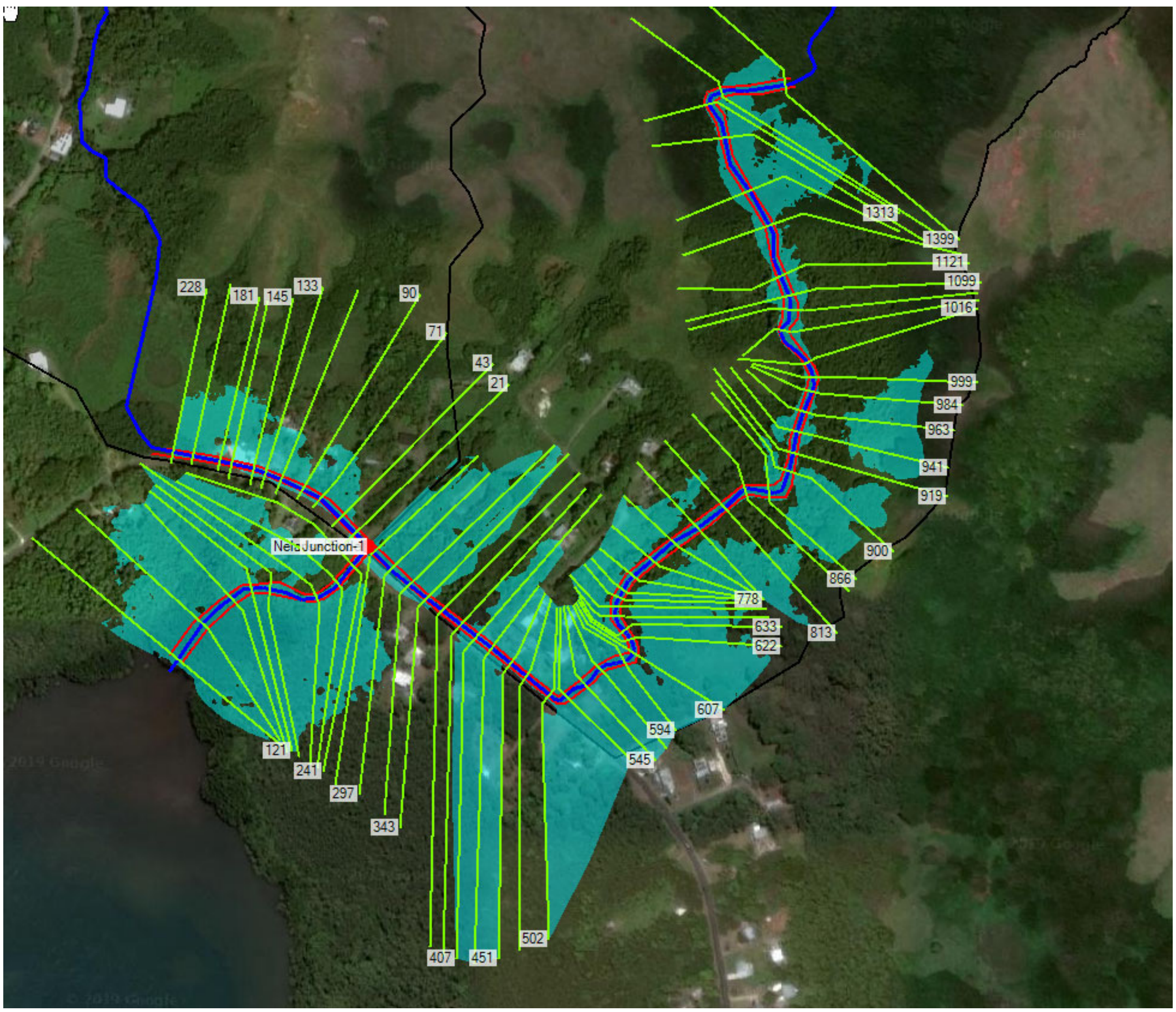

Figure 5-3: Inundated Areas in HEC-RAS for the 1% AEP (100-yr) Flood Event

onable amount. The bridge itself would overtop during the 1% AEP (100 year) event.

6. Flood Mitigation Alternatives

6.1 Reforestation

Frequent fires in the watershed have resulted in the native ravine forest being replaced with the more resilient and fire-adapted savannah grass. The impacts to the hydrology are summarized in this section with consideration toward re-establishment of the native vegetation as a potential flood mitigation alternative.

To begin, the runoff curve number (CN) for ravine forest and savannah grass are actually quite similar (55 and 58, respectively, on a scale of 0 to 100) (USDA, 1986). CN is an empirical parameter used in hydrology to characterize the runoff properties for a particular soil and ground cover. When comparing impacts to peak flow between savannah grass and ravine forest in a single instant or storm event, there is only a very mild increase when the cover is primarily savannah grass (Roose, Effects of Plant Cover, 1996). Bare soil, however, has a CN of 86 and would likely increase the peak flow and flood risk to the community significantly.

Savannah grass burns easily, but the roots remain alive and soon after an area burns over it sprouts again (Falanruw, Life on Guam: Savanna, Old Fields, Roadsides, 1976). Although the risk of fire and resulting bare soil is higher with savannah grass, its ability to quickly recover limits the time the soil is exposed. Small trees are often killed entirely when burned. In the short term, the savannah grass may be helping to reduce overland flow and sediment runoff by providing immediate cover to otherwise bare soil.

However, with each fire, the organic component of the soil is eroded and the ability for any type of vegetation to maintain its existence is lost, resulting in “badland” areas of bare soil. Even the savannah grasses would be unable to grow in these badland areas. Long term effects from burning and the creation of badlands are a real threat in terms of flood risk.

Other considerations that currently remain unanswered include the effectiveness of forested areas to limit the spread of fire and typical recovery times for re-establishment. Fires would likely spread more easily across dry savannah grass and burn a larger area.

For costing purposes, two reforestation scenarios shall be evaluated: 1 acre and 10 acres. Both sites are assumed to be adjacent to a main road, such as Route 2 or Jose Q. Aguon St, and planted with dominant tree species found in the local ravine forest already: hibiscus tiliaceaus, pandanus tectorius, pandanus dubius, ficus prolixa, glochidion marriannensis, and premna serratifolia (Liu & Fischer, 2006). The estimated cost of construction to reforest a 1 acre site is approximately $51,400 with a 43% contingency for a total estimated construction contract cost of $73,600.

6.2 **Restoring the Natural Flow Path of the Channel**

A historical topography map created by the U.S. Army, Army Map Service in 1944 (Army Map Service, 1944) shows the Nelansa (Manell) River flowing directly through Route 4 toward Balang Point (reference Figure 6-1 with the historical channel alignment highlighted in yellow). Currently, the Manell River makes a nearly ninety degree (90°) turn immediately upstream of Route 4 and runs parallel to this main road before crossing beneath it (reference Figure 6-2 with the current channel alignment highlighted in red). The intent of this proposed alternative is to restore the river to a somewhat natural flow path instead of forcing the water to make such a sharp turn in a developed area. While restoring it to its historical path exactly would require extensive work beyond what is necessary to reduce flood risk in the area, constructing a new culvert at the turning point and excavating through the bay front wetland to create a new outflow point would allow flood waters to drain from the area more effectively (reference Figure 6-2 with the proposed channel alignment in green).

The size of the culvert is proportionate with the size of the concrete channel upstream which has an area of approximately 8 m^2 (86 ft^2); reference Photo 6-1. The proposed culvert has a vertical span of 2 m (6.6 ft), span of 4 m (13 ft), and length/deck width of 6.4 m (21 ft). The headwall height (deck thickness) is approximately 0.8 m (2.6 ft).

Downstream of Route 4, a new channel would be excavated across the bay front wetland to create a new outflow point and allow flood waters to drain from the area more effectively. Regulatory and permitting actions should be limited as the proposed alternative is the *removal* of fill in the wetland rather than the *placement* of fill. The proposed channel is approximately 335 m (1,100 ft), trapezoidal shape with a base width of 6 m (20 ft), side slopes of 3H:1V, and depth of 1 m (3.3 ft). The approximate cut volume is 310 m^3 (11,000 ft^3).

It should be noted that this alternative by itself does not mitigate for the 1% AEP (100-year) peak discharge, which is approximately 96.6 m^3/s (3,410 ft^3/s) at this location. It was designed to be cost effective, but by doing so, only mitigates for the 20% AEP (5-year) event. It also assumes that the channel that runs parallel to Route 4 could still be utilized (left in place). The estimated cost of construction to restore the natural flow path of the channel is approximately $387,000 with a 35% contingency for a total estimated construction contract cost of $523,000.

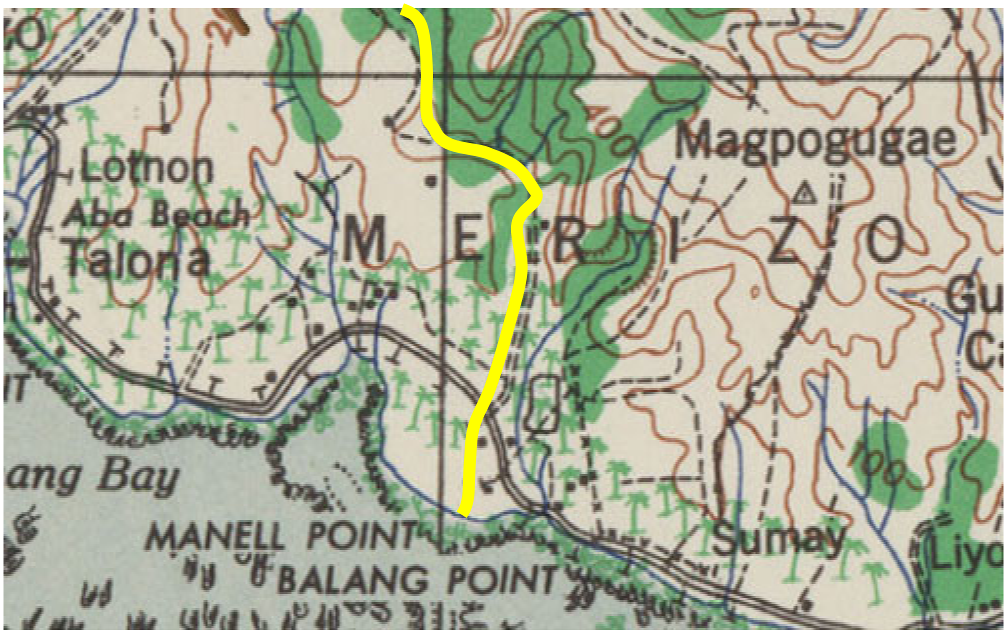

Figure 6-1: Historic Path of the Nelansa River

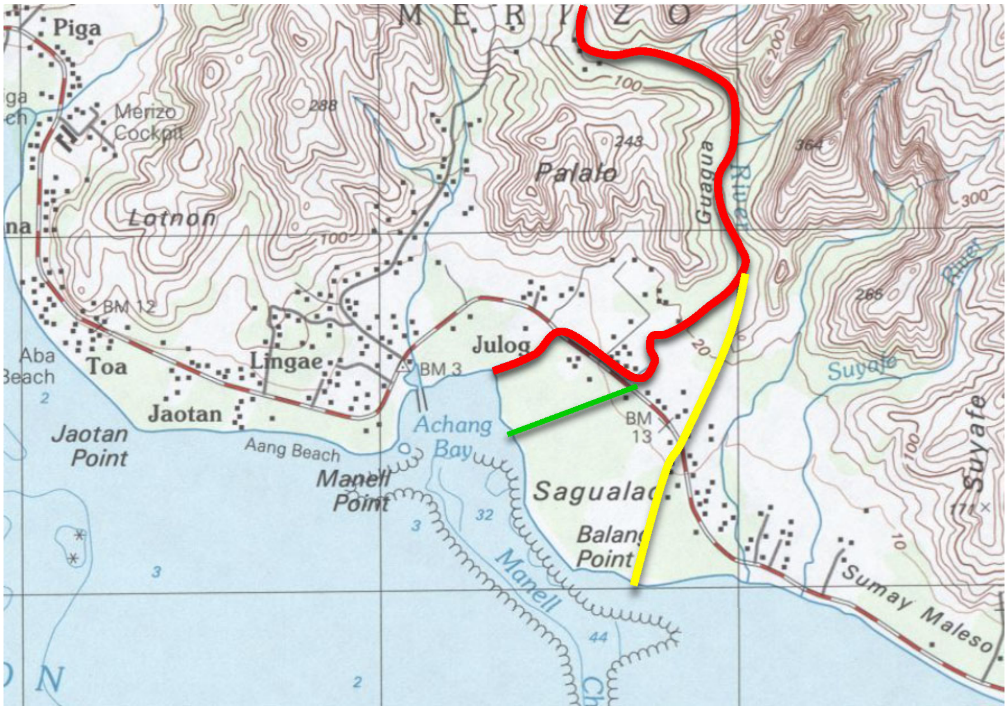

Figure 6-2: Current, Proposed, and Historical Path of the Nelansa River

Photo 6-1: Start of Concrete Channel Upstream of Route 4, Nelansa (Manell) River

6.3 **Upper Detention Basin**

Detention basins can be effective in reducing peak flow by capturing large amounts of water during a storm event and releasing it more gradually. In the Merizo Watershed, there are two possible locations for a detention basin: upstream of Route 4 along the Manell River and between Joutan Lane and J Baza Street. These locations are intended to capture flow from the Manell River and overland runoff from the mountains between the Manell River and Achang Bay, respectively.

Manell River Basin: To reduce flow along the Manell River, an in-stream detention basin is proposed at a site approximately 90 m (295 ft) upstream from Route 4 (see Figure 6-3) and along the Manell River. The areal extent, 0.027 km^2 (0.010 mi^2), was determined based on the existing channel alignment and topography. A depth of 1.5 m (4.9 ft), which is limited by the seasonally high groundwater table, would create an approximate volume of 40.5 m^3 (1,430 ft^3). This would contain nearly the 50% AEP (2 year) flood event and reduce the 10% AEP (10 year) peak flow in half.

Overland Runoff Basin: The terrain and aerial imagery indicates there are two existing detention basin between Joutan Lane and J Baza Street. It is unknown whether they are currently being utilized or are abandoned. These basins could be retrofitted to capture overland runoff from the nearby mountains and reduce the amount of flow entering the concrete ditch along Route 4. The drainage area for these basins are about 0.15 km^2 (0.06 mi^2). One basin has enough volume to contain the 50% AEP (2-year) storm; if both basins are utilized, they can contain the 20% AEP (5-year) storm. Grading and excavation to the basins themselves would be limited; however, a new swale or small channel will need to be cut to facilitate flow into the basins. The dimensions for the grassed, triangular swale are a depth of 1 m, height of 1 m, and length of 160 m. Additionally, a 0.9 m (3.0 ft) diameter corrugated culvert, approximately 20 m (66 ft) long, would be placed under J Braza Street. The estimated cost of construction to retrofit two detention basins is approximately $24,800 with a 43% contingency for a total estimated construction contract cost of $35,500.

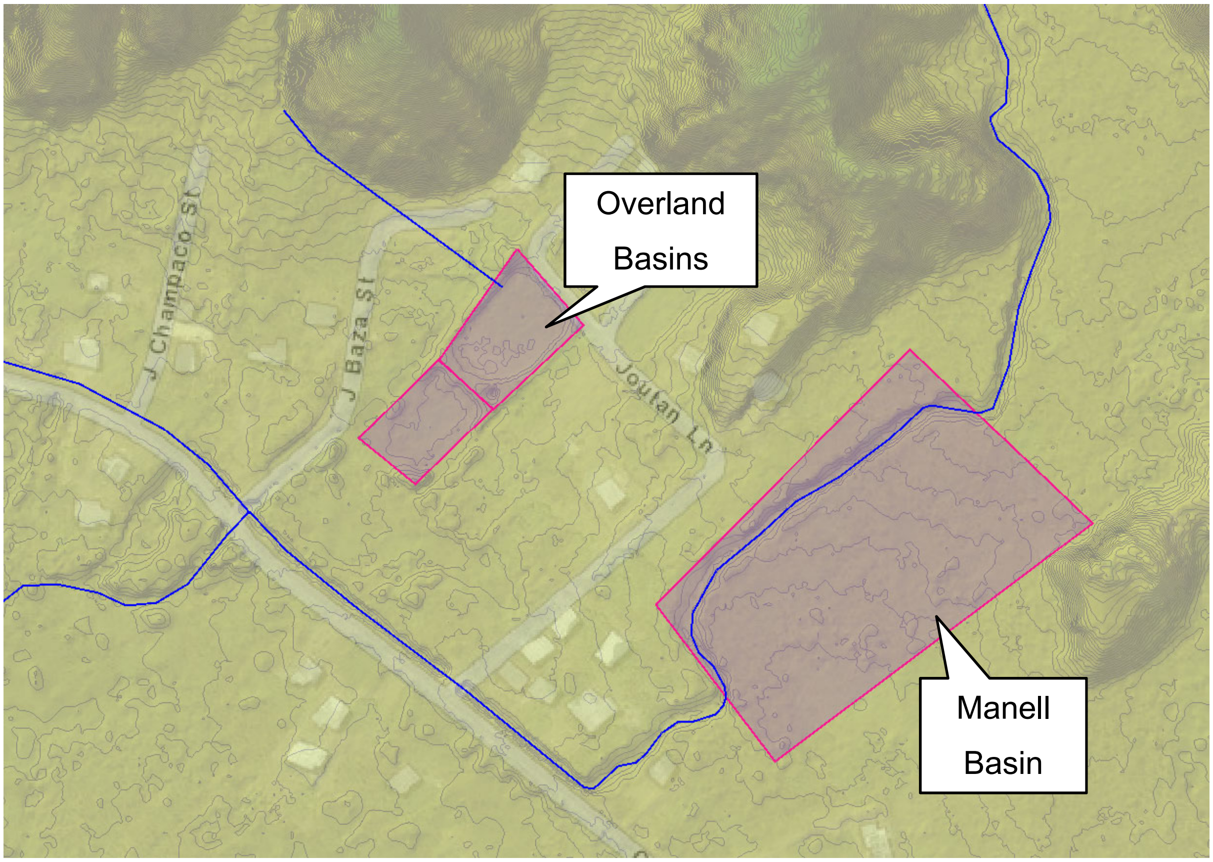

Figure 6-3: Potential Sites for a Detention Basin

7. References

Army Map Service. (1944). *Island of Guam*. Retrieved from University of Texas Libraries: http://legacy.lib.utexas.edu/maps/ams/guam/txu-pclmaps-oclc-6573395-island-of-guam.jpg

Falanruw, M. C. (1976). Life On Guam - Savanna, Old Fields, Roadsides. Territory of Guam: U.S. Office of Education - Department of Health, Education and Welfare. Retrieved from https://cnas-re.uog.edu/wp-content/uploads/2016/03/Life-on-Guam-Savanna-Old-Fields-Roadsides-2.pdf

Falanruw, M. C. (1976). *Life on Guam: Savanna, Old Fields, Roadsides*. Retrieved from University of Guam: https://cnas-re.uog.edu/wp-content/uploads/2016/03/Life-on-Guam-Savanna-Old-Fields-Roadsides-2.pdf

FEMA. (2007). *Flood Insurance Study.* Federal Emergency Management Agency.

Gingerich, S. B. (2003). Hydrologic Resources of Guam. Honolulu, Hawaii, USA: U.S. Department of the Interior, U.S. Geological Survey. Retrieved from USGS Publications Warehouse: https://pubs.usgs.gov/wri/wri034126/htdocs/wrir03-4126.html

Gingerich, S. B., Keener, V., & Finucane, M. L. (2015). Climate trends and projections for Guam. Honolulu, HI, USA: East West Center. Retrieved from https://www.pacificrisa.org/wp-content/uploads/2012/01/Pacific-RISA-Guam-flyer.pdf

Goodell, C. (2013, December 24). Lateral Structure Coefficients. Davis, CA, USA. Retrieved from http://hecrasmodel.blogspot.com/2013/12/lateral-structure-coefficients.html

Goodell, C. (2013). *Lateral Structure Coefficients*. Retrieved from The RAS Solution: http://hecrasmodel.blogspot.com/2013/12/lateral-structure-coefficients.html

Google Earth. (n.d.). Map of Guam. Retrieved from earth.google.com/web/

Heitz, L. F., & Khosrowpanah, S. (2015). *Prediction of Flow Duration Curves at Ungaged Sites in Guam.* Mangilao, Guam: Water and Environmental Research

Institute of the Western Pacific. Retrieved from https://guamhydrologicsurvey.uog.edu/

Interagency Advisory Committee on Water Data. (1982). *Bulletin #17B of the Hydrology Subcommittee.* Reston, VA: US Department of the Interior, Geological Survey, Office of Water Data Coordination. Retrieved from https://water.usgs.gov/osw/bulletin17B/dl_flow.pdf

Kottermair, M. (2012). *Piti-Asan Watershed Management Plan.* Mangilao, Guam: Water and Environmental Research Institute of the Western Pacific, University of Guam. Retrieved from http://www.weriguam.org/docs/reports/138.pdf

Lander, M. A., & Guard, C. P. (June 2003). *Creation of a 50-Year Rainfall Database, Annual Rainfall Climatology, and Annual Rainfall Distribution Map for Guam.* Technical Report No. 102. Mangilao, Guam: Water and Environmental Research Institute of the Western Pacific, University of Guam. Retrieved from http://www.weriguam.org/docs/reports/102.pdf

Liu, Z., & Fischer, L. (2006). Guam Vegetation Mapping Using Very High Spatial Resolution Imagery. McClellan, CA, USA: United States Department of Agriculture, U.S. Forest Service. Retrieved from U.S. Forest Service: https://www.fs.usda.gov/Internet/FSE_DOCUMENTS/fsbdev3_046054.pdf

Merizo, Guam. (2019). Retrieved from LatLong.net: https://www.latlong.net/place/merizo-guam-951.html

Moriasi, D. N., Arnold, J. G., Van Liew, M. W., Bingner, R. L., Harmel, R. D., & Veith, T. L. (2007). Model Evaluation Guidelines for Systematic Quantification of Accuracy in Watershed Simulations. *Transactions of the ASABE, 50(3): 885-900*. American Society of Agricultural and Biological Engineers. doi:0001-2351

National Oceanic and Atmospheric Administration. (2017, June 20). Datums for 1630000, Apra Harbor, Guam. Apra Harbor, Territory of Guam, USA. Retrieved from https://tidesandcurrents.noaa.gov/datums.html?id=1630000

National Weather Service. (2017, April 21). NOAA Atlas 14 Point Precipitation Frequency Estimates. Silver Spring, MD, USA: US Department of Commerce, National Oceanic and Atmospheric Administration, National Weather Service. Retrieved from https://hdsc.nws.noaa.gov/hdsc/pfds/pfds_map_pi.html

National Weather Service. (2017, April 21). *NOAA ATLAS 14 POINT PRECIPITATION FREQUENCY ESTIMATES*. Retrieved from Hydrometeorological Design Studies Center Precipitation Frequency Data Server (PFDS): https://hdsc.nws.noaa.gov/hdsc/pfds/pfds_map_pi.html

Natural Resources Conservation Service. (1986). Urban Hydrology for Small Watersheds, TR-55. United States Department of Agriculture, Natural Resources Conservation Service. Retrieved from https://www.nrcs.usda.gov/Internet/FSE_DOCUMENTS/stelprdb1044171.pdf

NOAA. (2017). *NOAA Atlas 14 Point Precipitation Frequency Estimates*. Retrieved from NOAA'S National Weather Service: https://hdsc.nws.noaa.gov/hdsc/pfds/pfds_map_pi.html

NOAA. (2018). *Datums for 1630000, Apra Harbor, Guam* . Retrieved from NOAA: https://tidesandcurrents.noaa.gov/datums.html?id=1630000

NOAA. (n.d.). *Datums for 1630000, Apra Harbor, Guam*. Retrieved from Tides & Currents: https://tidesandcurrents.noaa.gov/datums.html?id=1630000

Roose, E. (1996). *Effects of Plant Cover.* Retrieved from Food and Agriculture Organization of the United Nations: http://www.fao.org/docrep/t1765e/t1765e0h.htm

Roose, E. (1996). Land husbandry - Components and strategy. Rome, Italy: Food and Agriculture Organization of the United Nations, Soil Resources Management and Conservation Service Land and Water Development Division. Retrieved from http://www.fao.org/docrep/t1765e/t1765e0h.htm

Soil Conservation Service. (1985). *Soil Survey of Terriotry of Guam*. Retrieved from https://www.nrcs.usda.gov/Internet/FSE_MANUSCRIPTS/pacific_basin/PB640/0/guam.pdf

Soil Conservation Service. (1985). Soil Survey of Territory of Guam. Territory of Guam, USA: United States Department of Agriculture, Soil Conservation Service. Retrieved from https://www.nrcs.usda.gov/Internet/FSE_MANUSCRIPTS/pacific_basin/PB640/0/guam.pdf

Stark, J. T. (1963). Petrology of the Volcanic Rocks of Guam. United States Government Printing Office, Washington, USA: United States Department of the Interior, Geological Survey. Retrieved from https://pubs.usgs.gov/pp/0403c/report.pdf

University of Guam. (2016, February 16). *Soils of Guam*. (USDA Natural Resources Conservation Service) Retrieved from Research & Extension: https://cnas-re.uog.edu/soils-of-guam/?where-found%5B%5D=Merizo&soil-name%5B%5D=Inarajan+series&wpv_aux_current_post_id=3244&wpv_view_count=3243-TCPID3244

University of Guam. (2016). *Soils of Guam*. Retrieved from Research & Extension: https://cnas-re.uog.edu/soils-of-guam/?where-found%5B%5D=Merizo&soil-name%5B%5D=Agfayan+series&wpv_aux_current_post_id=3244&wpv_view_count=3243-TCPID3244

University of Guam. (2016). *Soils of Guam*. Retrieved from Research & Extension: https://cnas-re.uog.edu/soils-of-guam/?where-found%5B%5D=Merizo&soil-name%5B%5D=Inarajan+series&wpv_aux_current_post_id=3244&wpv_view_count=3243-TCPID3244

USACE. (1980). *Flooding and Drainage on Guam.* Fort Shafter, HI: United States Army Corps of Engineers, Honolulu District.

USACE. (1982). *Alternative Solutions for Flood Prone Areas in Guam.* Fort Shafter, HI: US Army Corps of Engineers, Pacific Ocean Division.

USACE. (1983). *Alternative Solutions for Flood Prone Areas in Guam.* Fort Shafter, HI: US Army Corps of Engineers, Honolulu District.

USDA. (1986). *Urban Hydrology for Small Watersheds TR-55*. Retrieved from United States Department of Agriculture: https://www.nrcs.usda.gov/Internet/FSE_DOCUMENTS/stelprdb1044171.pdf

USGS. (n.d.). *USGS Surface-Water Data for the Nation*. (US Department of the Interior, US Geological Survey) Retrieved from National Water Information System: Web Interface: https://nwis.waterdata.usgs.gov/nwis/sw

WERI and IREI. (n.d.). *Digital Atlas of Southern Guam*. Retrieved from HydroGuam.net: http://south.hydroguam.net/

WERI and IREI. (n.d.). *Digital Atlas of Southern Guam*. (Water and Environmental Research Institute of the Western Pacific and Island Research & Education Initiative) Retrieved from HydroGuam.net: http://south.hydroguam.net/geographic-geology.php

Wong, M. F. (2010). Guam Flood Frequency Regional Regression Equations. US Army Corps of Engineers, Honolulu District.